RESEARCH ARTICLE

DOI: 10.54392/irjmt2559

INTERNATIONAL RESEARCH JOURNAL OF MULTIDISCIPLINARY TECHNOVATION

Asian Research Association

A Compact Design and Development of WBAN Textile Antenna for WLAN, WiMAX and IOT Applications

Parisa BoseBabu [a,*], P.A. Nageswara Rao [b]

[a] AU-TDR HUB, Andhra University, Visakhapatnam-530003, India.

[b] GVP College for Degree & P.G Courses (A), Visakhapatnam-530045, India.

* Corresponding Author Email: pbosebabu@gmail.com

DOI: https://doi.org/10.54392/irjmt2559

Received: 02-06-2025; Revised: 28-08-2025; Accepted: 09-09-2025; Published: 28-09-2025

Abstract: This paper presents triple-band antenna design geometry for textile antenna applications. The proposed antenna utilises the inherent conformal features of Jeans as the substrate and a conducting surface with flexible metal as the radiating surface. The proposed antenna geometry is simple in structure yet complicated in dimensions as it is susceptible to radiation characteristics. The proposed triple band antenna covers the operating frequency ranges notably, 2.3183-2.4465 GHz (128 MHz), 3.2240 GHz-3.9902 GHz (Bandwidth of 766 MHz) and 5.1858-5.6042 GHz (Bandwidth of 418 MHz). The bands of operation are suitable for WLAN, WiMAX and IoT applications respectively. The final outer dimensions of the proposed compact triple band antenna is 20 mm x 50 mm x 0.254 mm with Jeans of thickness of 10 mils (0.254 mm) used as the substrate. The triple band antenna is modelled on the efficient CAD tool embedded in the CST in which the simulations are carried out and analysis is performed using the generated reports like reflection coefficient, VSWR and radiation patterns. The simulations and measurement results are good agreement in terms of bandwidth (BW), Return Loss (S11) and Radiation pattern (RP), bending analysis and Specific Absorption rate (SAR).

Keywords: Triband antenna, Textile antenna, WLAN, WiMAX, IoT

1. Introduction

Wearable antennas have become an essential component of WBANs (wireless body area networks), which are widely utilized in healthcare, business, military, entertainment, and other applications [1-2]. Typically, these antennas are worn directly on the human body and commonly integrated into garments/cloths, helmet mounted or wrist worn [3–5]. However, the high dielectric constants and non-uniform characteristics of various human tissues significantly affect the performance of wearable textile antennas. Additionally, wearable textile antennas can impact the human body, necessitating compliance with safety standards, often evaluated through specific absorption rate (SAR) values.

Wearable antennas have emerged as one of the most promising technologies for WBANs enabling applications across healthcare monitoring, Internet of Things (IoT), Defence communications and personal electronics. A key challenge in these systems is ensuring compact size, multi band operations, stable performance under body loading conditions and reduced SAR to minimize radiation exposure to human tissues. Traditional antennas are more effective in narrowband scenarios and has limitations in terms of bandwidth, radiation efficiency and safety compliance when they are integrated into wearable devices.

To overcome these challenges researchers turned to metamaterial (MTM) structures provides unique electromagnetic properties not available in conventional materials. By carefully engineering subwavelength unit cells MTMs such as artificial magnetic conductors (AMCs), electromagnetic bandgap (EBG) structures, and metamaterial surfaces (MS) can improve antenna performance in wearable scenarios. These structures are particularly effective at reducing back radiation toward the human body, improving forward gain and controlling current distributions thereby enhancing both efficiency and user safety.

This literature survey critically reviews the evolution of metamaterial loaded wearable antennas, beginning with single band AMC systems that progressing to dual band and EBG integrated antennas and finally expanding to multi-band and wideband designs that aim to meet the growing demands of WBAN applications. AMC structures are one of the most widely studied metamaterial configurations for wearable antenna design. AMCs function as in-phase reflectors,

enabling antennas to achieve high front-to-back ratios while minimizing back lobe radiation toward the body.

In [6, 7] discussed about single band AMC backed wearable antennas. These designs demonstrated significant SAR reduction by positioning the AMC layer beneath the radiating patch redirected electromagnetic waves away from the human body. The AMC layer also improved impedance matching enabling stable operation near body tissues. However, the designs were primarily limited to single frequency operation, which restricts their utility in multi standard communication systems. The main advantages of AMC-loaded antenna consist of reduced SAR, increasing gain and compact integration. The limitation is narrowband operation inadequate as WBAN applications and demand for multi-band operations (e.g., Bluetooth, WLAN, WiMAX, and sub-6 GHz 5G).

EBG structures are another class of metamaterials that suppress surface waves enhancing radiation efficiency and isolation. The AMCs primarily act as reflectors, EBGs also offer bandgap characteristics that help suppress unwanted resonances and improve multi band performance.

In [8, 9], researchers presented dual-band EBG-loaded wearable antennas. These designs targeted WBAN applications such as healthcare monitoring and wireless communications by offering operation at two distinct frequency bands. The dual-band capability provided flexibility for supporting multiple standards, while the EBG layer reduced surface wave losses and body induced detuning effects.

The EBG loaded antennas advantages are dual band operation, suppression of surface waves and angular stability. Despite these advantages, dual-band EBG-based designs still fall short of supporting multi band or wideband operations which is increasingly necessary for future WBAN devices.

The MS structures represent a general class of MTM inspired designs used to improve antenna performance. In [10], a wearable antenna incorporating an MS structure was introduced. The MS layer provided enhanced control of the electromagnetic field distribution leading to improved impedance matching and SAR reduction. The MS loaded antennas offer flexibility in design and improved safety performance, they generally remain limited to one or two frequency bands, continuing the trend observed with AMC and EBG based solutions.

The existing literature on AMC, EBG and MS loaded antennas highlights significant progress in SAR reduction, gain enhancement and wearable integration. However, these approaches share a common limitations like single/dual band operations. The growing demand for multi-functional wearable devices, there is an urgent need for antennas that can operate at multiple frequency bands simultaneously without compromising compactness, flexibility and user safety.

Recent studies have shifted focus toward multi-band and wideband wearable antennas to address the shortcomings of single and dual band metamaterial loaded designs. These antennas are particularly valuable in WBANs, where different medical and IoT applications require connectivity across diverse frequency ranges.

In [8, 9, 11, 12] proposed dual band textile antennas incorporating metamaterial loading. Textile based implementations offer advantages in terms of flexibility, lightweight integration, and comfort for wearable applications. However, dual band designs are insufficient when multiple frequency bands must be covered. To extend the coverage various researchers have introduced triple-band wearable antennas. In [13], reported a design using grooves on the ground plane and a Hilbert shape radiating element. The work supported operation across three frequency bands and demonstrating the potential of geometric modifications for achieving multi band functionality. Similar work presented in [14], a compact button antenna operating at 0.867, 2.35 and 5.85 GHz. The form factor made it attractive for integration into clothing and small wearable devices.

To further enhance frequency coverage, researchers have also introduced triple-band and multi-band wearable antennas [13–18], providing greater versatility for next-generation WBAN applications. A triple band antenna with grooves on ground plane and Hilbert shape on the top layer is design and developed in [13]. In [14], a compact button antenna is with compact structure is operating in the frequencies 0.867, 2.35 and 5.85 GHz is developed. An open ring triband dual polarization antenna sued for medical applications as well as intelligent internet is realized in [15]. A CPW slot dipole antenna for WBAN applications is realized in the frequencies of WLAN applications i.e, 2.4/5.2/5.8 GHz, WiMAX band i.e., 3.5 GHz and C-band of 4.4 GHz is developed in [17].

In this paper, a low profile and compact WBAN triple band on-body jeans material antenna is designed and developed for WLAN, WiMAX and IOT applications. The proposed compact triple band antenna impedance bandwidth, reflection coefficient, radiation parameters are analyzed in this paper. This work is organized as follows, the proposed antenna structure for triple band antenna is analyzed in the section 2. The simulation and measured results of proposed triple band structure is presented in the section 3 and 4 respectively. The performance comparison of the proposed triple band antenna with previous literature and overall conclusion of the paper is represented in section 5.

2. Literature Review

The literature work carried out by various researchers are tabulated in below table 1.

Table 1. overview of literature

Reference	Key Findings / Contributions	Limitations / Remarks
Seyedi *et al*. [1]	Provided comprehensive survey of intrabody communication technologies	Lacked practical antenna design aspects
Seneviratne [2]	Energy efficiency, antenna miniaturization and integration	More focused on general wearables, limited antenna specifics
Ashyap *et al*. [3]	Demonstrated effectiveness of EBG in wearable antennas	Fabrication complexity effects not detailed.
Song & Rahmat-Samii [4]	Showed deformation impacts resonance, gain & SAR	Limited to rectangular patch; other geometries unexplored
Singh *et al*. [5]	Achieved high near-field performance for RFID technology	Focused on RFID, not broadband WBAN
Agarwal *et al.* [6]	Improved efficiency & SAR reduction	Latex substrate less practical for mass production
Alemaryeen & Noghanian [7]	Achieved compact, flexible and SAR-reduced design	Mechanical durability under stress not addressed
Velan *et al.* [8]	Achieved dual-band wearable antenna with reduced SAR	Bandwidth improvement still needed
Gao *et al*. [9]	Stable response & low SAR demonstrated	Narrowband performance

3. Proposed triple band Design

Typical geometry consists of a rectangular jeans substrate with a εr of 2 and a thickness 0.254 mm. The radiating patch is placed on the surface with a specific shape and pattern, while the ground is arranged as a truncated rectangular slot on the other side of the substrate known as Defected Ground Structure (DGS). The DGS introduces a localized disturbance in the ground, which alters the current distribution and input impedance of the antenna. This helps in fine-tuning the impedance characteristics, leading to improved $|S_{11}|$ response and broader impedance bandwidth. The radiating surface is formed by connecting rectangular microstrip lines with the desired radiation pattern. Start with a horizontal long microstrip line is arranged on the radiating side precisely normal to the feed line in such a way that the field line touches this horizontal microstrip line precisely at the centre. Two vertical microstrip lines of different lengths are arranged on either edge of this horizontal line. Towards the left edge, a shorter microstrip line is arranged wild; towards the right edge, the vertical line is almost double in size. The top edges of these two vertical lines are again provided with horizontal microstrip lines individually. However, the horizontal lines arranged on top of these two vertical lines have different widths. The one placed on the left vertical line is wider than the one on the right. Also, the position of the placement of these horizontal lines is different concerning each other. For instance, the broad horizontal line towards the left is placed asymmetrically in such a way that its centre lies away from the vertical line towards the left; however, the horizontal line lying on the top of this right vertical line is placed exactly centre search that it appears symmetrical on either direction. The whole geometry constitutes the radiating surface, which is fed using an edge feed run from the long edge of the substrate to the centre of the first horizontal line. The ground plane is not completely enhanced partially, known as a defective ground, and it just comprises a wider microstrip line that runs along the length of the long side of the substrate with a width less than that of the substrate's width. The initial design pertaining to this discussion is shown in Figure 1.

The designed patch is further modified in order to accommodate one more band of operation. The modifications involve extending the existing design. The horizontal line placed on top of the vertical line towards the left was modified for the desired response. The modification has a vertical line at the edge of this horizontal line, which is again extended towards the right horizontally to form a U shape, which is asymmetrical. The U shape is horizontal; as mentioned, it is asymmetrical, with two arms of different lengths. The arm on the top is slightly lengthier than the arm's lower side. Also, the arm on the top has a short vertical microstrip line running from its edge. This modified geometry is presented in Figure 2. The optimised dimensions of the triple band antenna are represented in Table 1. Although the geometry looks simply, it is characterised by several dimensions and notations, so designing this antenna is always complicated. Any slight deviation in terms of the dimensions or the geometry will differ in its radiation characteristics and bands of operation.

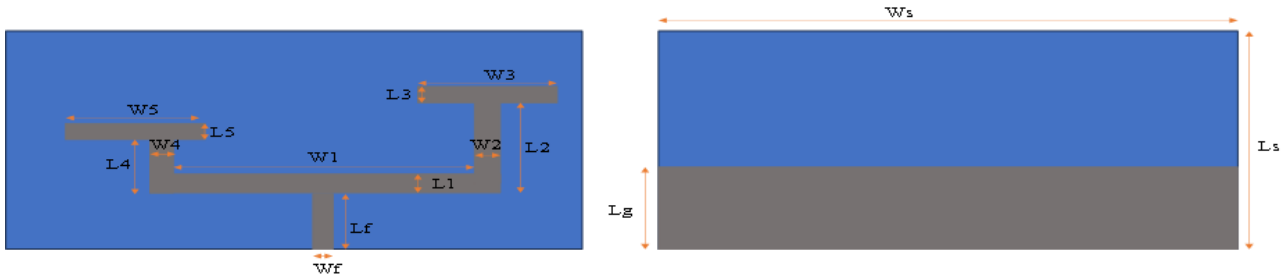

Figure 1. Initial Design for Dual band

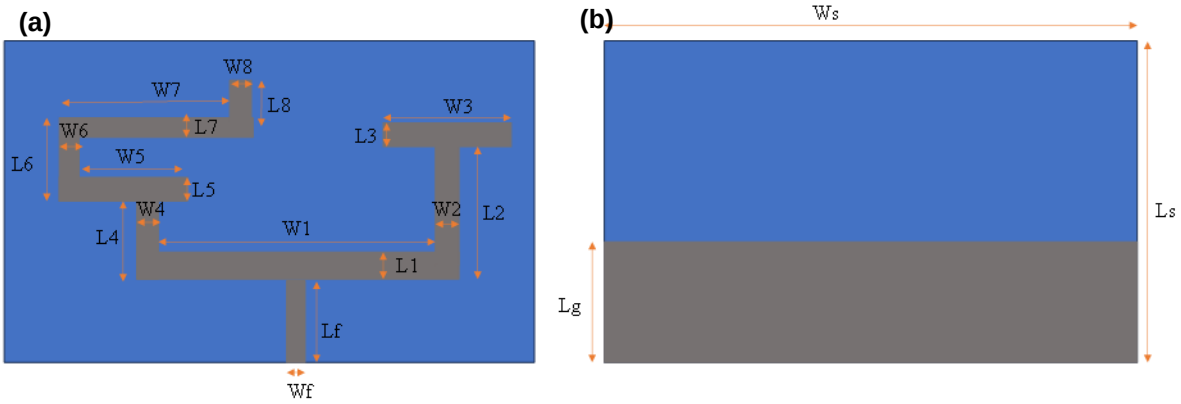

Figure 2. Proposed compact triple band Antenna (a) Front view (b) Rare view (Ground)

Table 1. Triple Band antenna design Parameters

S. No	Parameter	Value in mm
1	Ls	20
2	Ws	50
3	H	0.254
4	Lg	5
5	T	0.035
6	Lf	4.3
7	Wf	0.8
8	W1	15.8
9	L1	0.3
10	W2	0.3
11	L2	10
12	W3	4
13	L3	1.5
14	W4	0.3
15	L4	3.1
16	W5	10
17	L5	2
18	W6	1
19	L6	3.6
20	W7	12.8
21	L7	1.3
22	W8	1
23	L8	2

To analyse the same, it is significant perform parametric analysis. The simulations are carried out in the commercially available CST studio suite with mesh size of 1 mm x 1 mm. The Perfect Electric Conductor (PEC) boundaries are taken for the simulation of the proposed design. The FDTD solver used for the better accuracy of the system.

4. Simulation Results

Further, to analyse the characteristics of the proposed compact triple band antenna design, it is

essential to simulate some standard evaluating parameters in terms of radiation and electrical features known as reflection coefficient and VSWR plots and the field distribution plot. To start with a simple single-band operation, characteristics expressed by the rectangular patch are analysed. The analysis includes the reflection coefficient plot presented in the Figure 3. It is observed from the simulation results that the antenna radiates around the operating bands of 2.3183-2.4465 GHz (Bandwidth of 128 MHz), 3.2240 GHz-3.9902 GHz (Bandwidth of 766 MHz) and 5.1858-5.6042 GHz (Bandwidth of 418 MHz).

As discussed in the triple band antenna design section, the antenna design seems to be quite simple however very sensitive to any dimensional variations. To analyse the effect of dimensional variations on the radiation characteristics of the triple band antenna, parametric analysis has been performed in terms of Ws, L1, W1, L2, L3, W3, L4, L5, and W5. These dimensional parameters are varied over a wide range of values, following which the respective radiation characteristics in terms of S11 one is plotted.

For instance, Ws is varies from 45-55 mm with an interval of 5 mm with 3 different readings and the corresponding S11 and VSWR are plotted and presented in figure 3(a) and 3(b). Though the dual resonant characteristics have not changed as per the plots, there is a significant variation in the intermediate/middle band which has a minor contribution in terms of reflection coefficient and BW. As the Ws is increasing this minor band is moving towards the first significant resonant band.

Further, the parametric analysis based on L1 (0.2, 0.3, 0.4 mm), W1 (14.8, 15.8, 16.8 mm), L2 (9, 10, 11 mm), L3 (1, 1,5, 2 mm), W3 (3, 4, 5 mm), L4 (2.1, 3.1, 4.1 mm), L5 (1, 2, 3 mm) and W5 (9, 10, 11 mm) with the respective values and their respective radiation characteristics in terms of S11 are presented in figure 4(a) through 4(h).

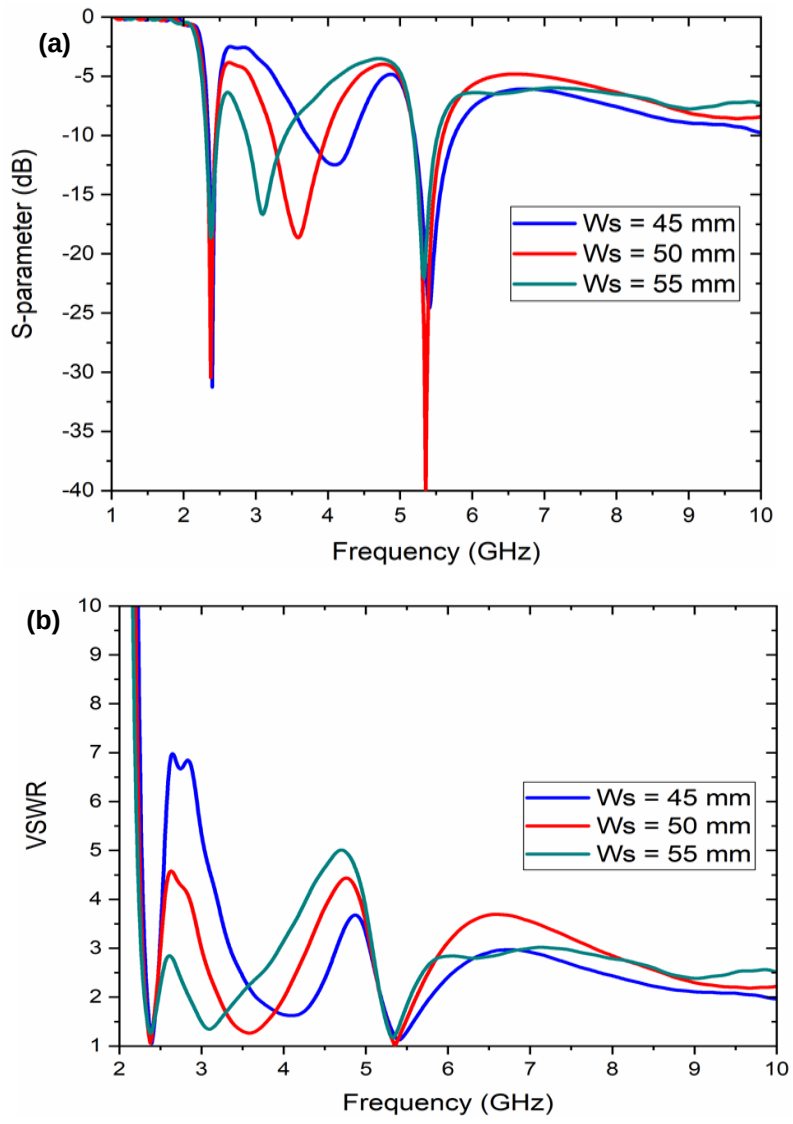

Figure 3. Simulation results of proposed triband antenna by varying the Ws parameter (a) Return Loss (S11) and (b) VSWR

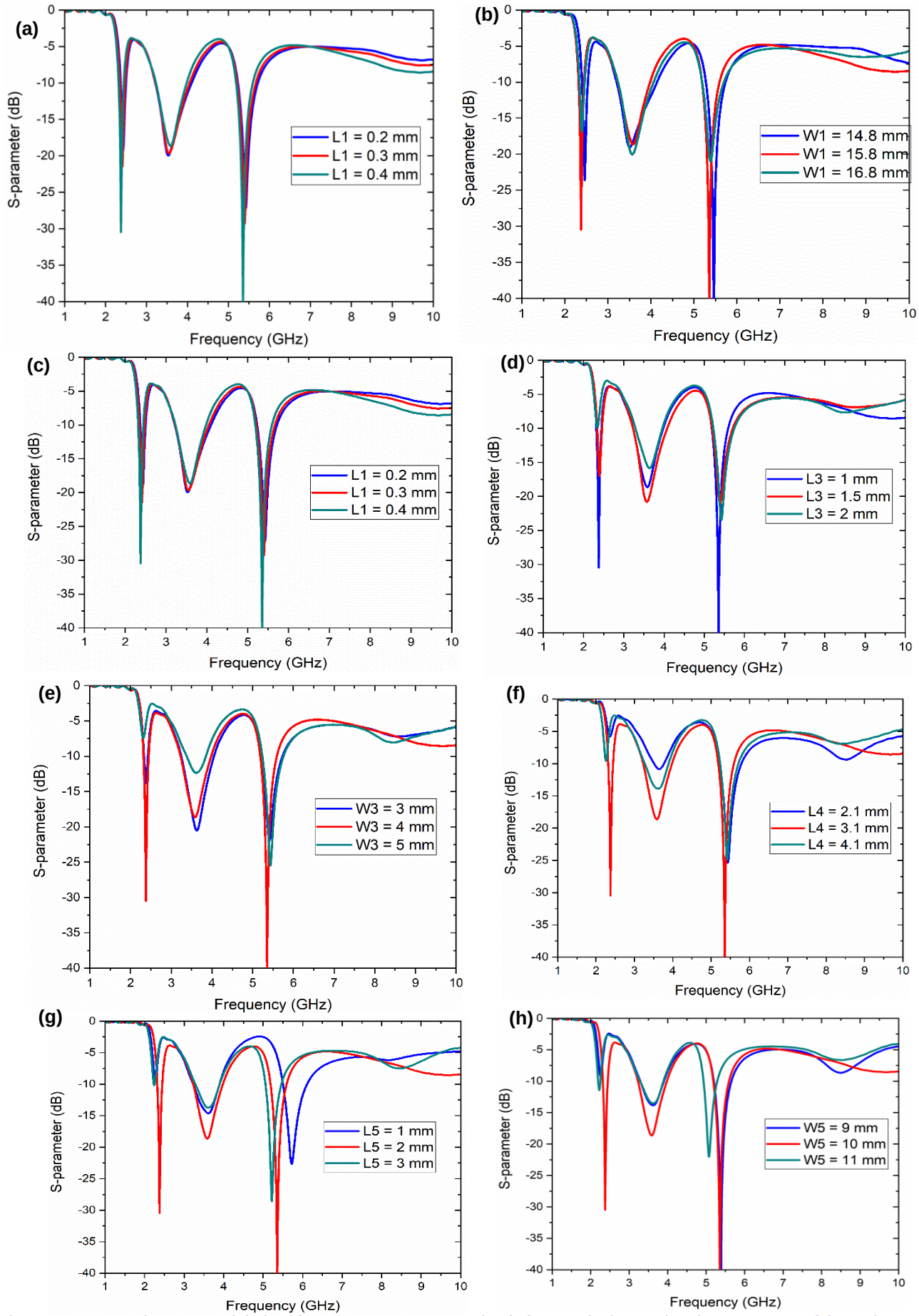

Figure 4. Proposed compact triple band antenna S-parameter simulation results by varying the parameters **(a)** Varying L1 parameter **(b)** Varying W1 parameter. **(c)** Varying L2 parameter **(d)** Varying L3 parameter **(e)** Varying W3 Parameter **(f)** Varying L4 parameter **(g)** Varying L5 parameter **(h)** Varying W5 parameter

It can be inferred from the S11 plots that the impact of these physical dimensions is not significant, as there is no evidence of variation in the resonant bands. However, we see that in the second considerable band as well as the first and intermediate bands, the respective S11 is decreasing with increasing dimensional value. However, there is a noticeable impact bye L4, L5, and W5 on the frequency response and they respective president frequencies. As their values of these dimensions are increased is significant shift in the first and the second significant bands towards left is observed.

In order to figure out the radiation pattern characteristics and its distribution it may be of interest to analyse the respective field distributions and the surface current distribution on the radiating surface. Taking this into consideration plots describing the E-field distribution at the 3 different resonant bands namely 2.4, 3.5, 5.5 GHz are simulated and presented in figure 5(a), (b) and (c) respectively. Similarly, the H-field distribution plots are presented in figure 6(a), (b) and (c) respectively for the frequencies 2.4, 3.5 and 5.5 GHz. Both the Enfield and H field distribution plots are in good agreement at the respective resonant frequencies contributing to similar radiation characteristics. Further, the current distribution graphical plot is presented in Figure 7(a) through Figure 7(c), In which it is evident that the distribution is dense in the direction of strong field. The surface current distribution demonstrates how the surface current intensity and path are altered due to frequency change are directly linking the electromagnetic behavior.

For the identified 3 resonant frequencies on the 3 resonant bands, the respective radiation patterns in both 3-dimensional and 2-dimensional are simulated and presented in Figure 8(a) through Figure 8(i). The radiation patterns, especially from the 3D plots, make it evident that the maximum radiation is concentrated in one direction.

The planner plots all the 3 bands in XY cut and YZ cut have similar shape in terms of distribution pattern. The gain and beam width are measured from these plots and tabulated in Table 2 against the 3 resonant frequency bands**.**

5. Measured Results

For better validation, the simulated antenna's respective geometry has been fabricated, and a prototype has been developed. The fabricated prototype is presented in Figure 9. This helps us perform some measurements, which are real-time values of the proposed characteristics. These measurements include VSWR and reflection coefficient. The measurement setup further S11, VSWR and the radiation pattern is shown in the photographs presented in Figure 10 (a), (b) and (c), respectively. The screenshot taken from the network analyser while measuring the return loss (S11) is presented in Figure 11. It is interesting to see that respective measured results of the fabricated triple band antenna are in good agreement with simulation results, which is evident because of the simple geometrical structure, yet complicated in terms of dimensional sensitivity proposed antenna design.

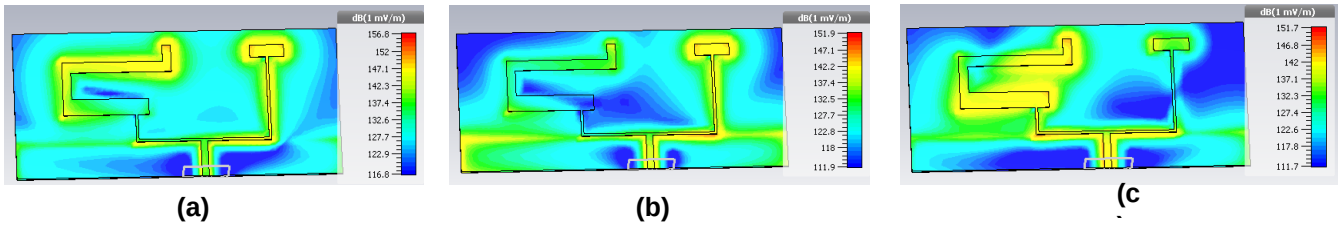

Figure 5. E filed Distributions at frequencies (a) 2.4 (b) 3.5 and (c) 5.5 GHz

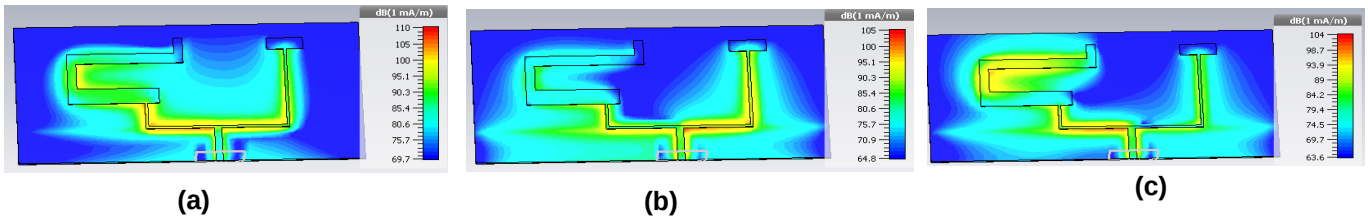

Figure 6. H-field Distributions at frequencies **(a)** 2.4 **(b)** 3.5 and **(c)** 5.5 GHz

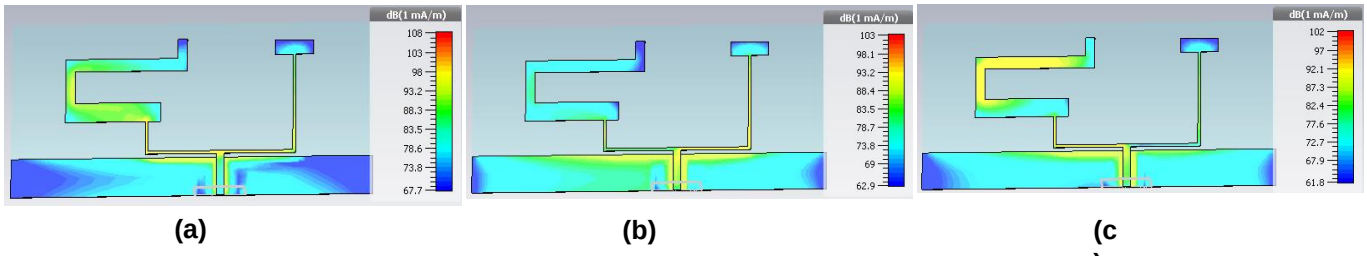

Figure 7. Surface current distributions **(a)** 2.4 **(b)** 3.5 and **(c)** 5.5 GHz

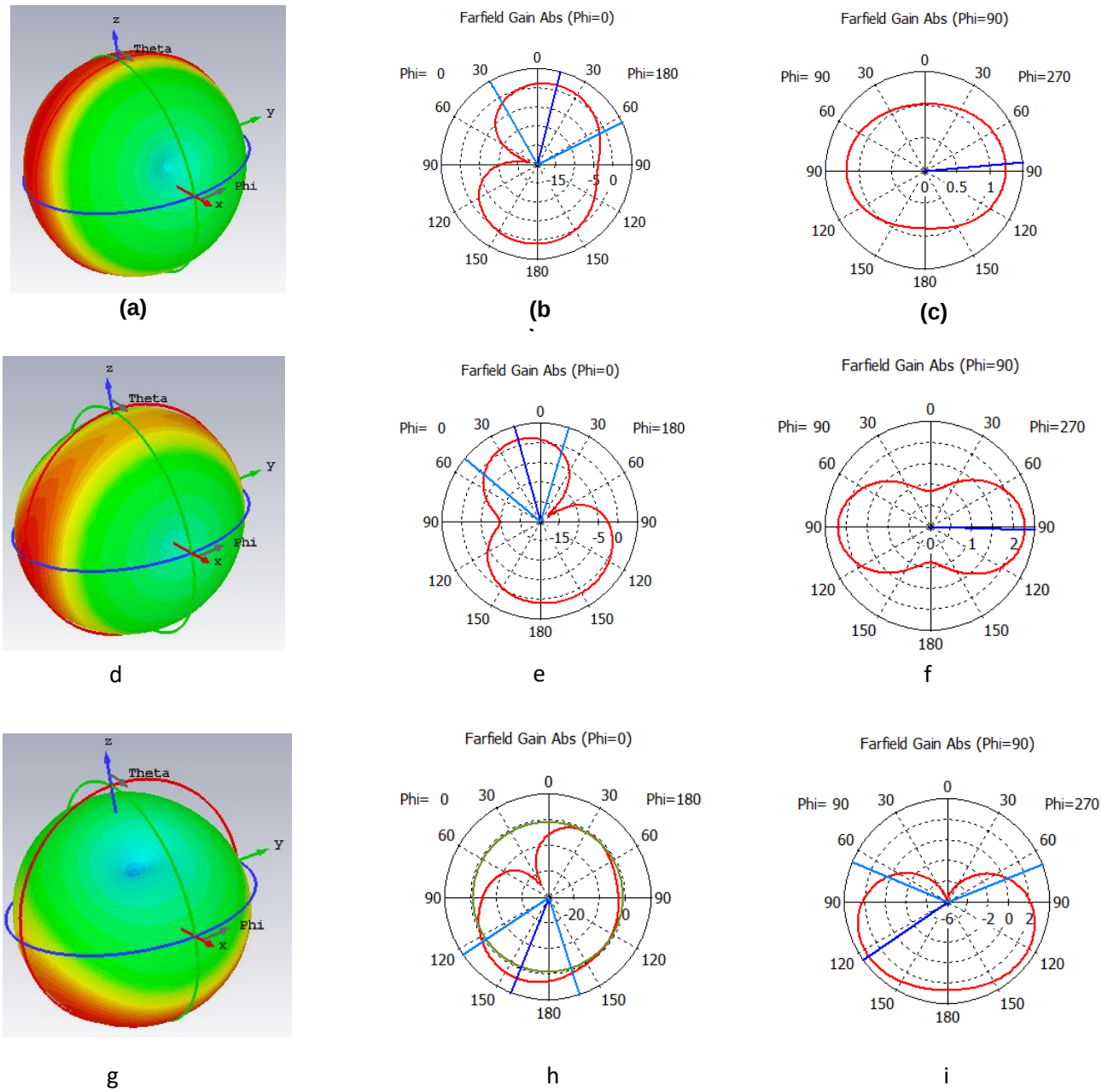

Figure 8. (a), (d) and **(g)** are 3D radiation pattern of the proposed compact triple band antenna at 2.4, 3.5 and 5.5 GHz respectively. **(b), (e)** and **(h)** are 2D radiation pattern with phi =0 degrees at 2.4, 3.5 and 5.5 GHz. **(c), (f)** and **(i)** are 2D radiation pattern with phi =90 degrees at 2.4, 3.5 and 5.5 GHz respectively.

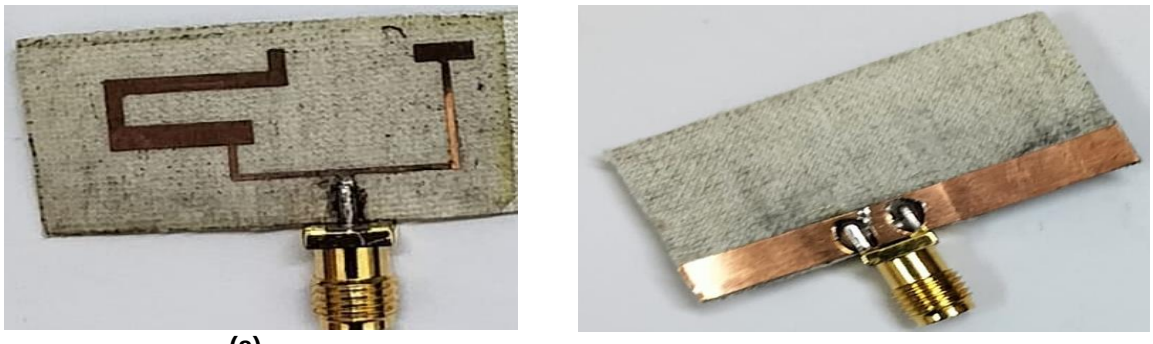

Figure 9. Fabricated prototype of the proposed antenna (a) Front view (b) ground plane

Table 2. Radiation characteristics

S. No	Frequency (GHz)	Gain (dB)	Beamwidth (deg)
1	2.4	1.28	93.8
2	3.5	1.46	67.4
3	5.5	3.69	73.5

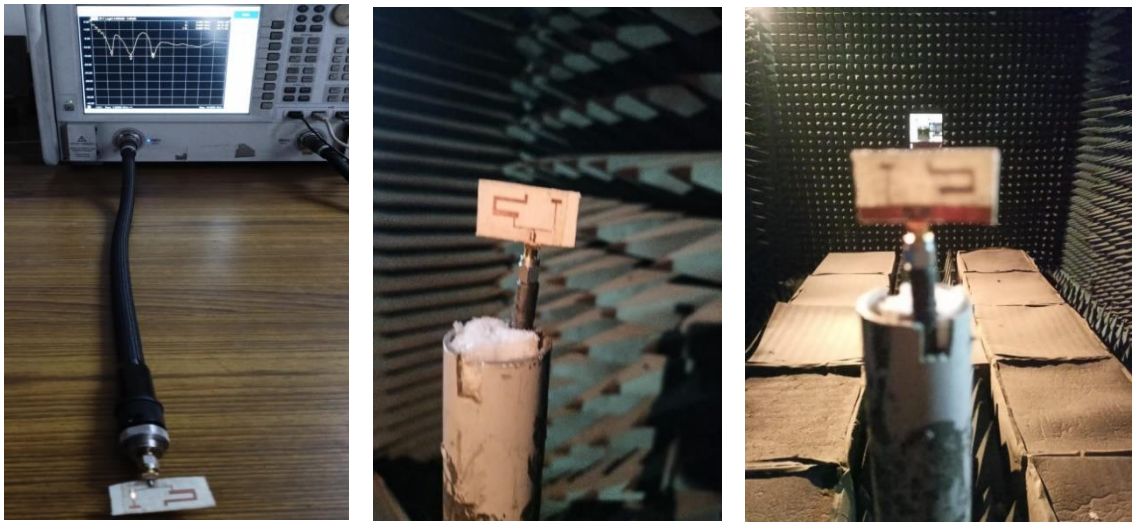

(a) (b) (c)

Figure 10. Measurement setup (a) Reflection coefficient (b) Mounted DUT on Anechoic Chamber (c) Radiation pattern setup

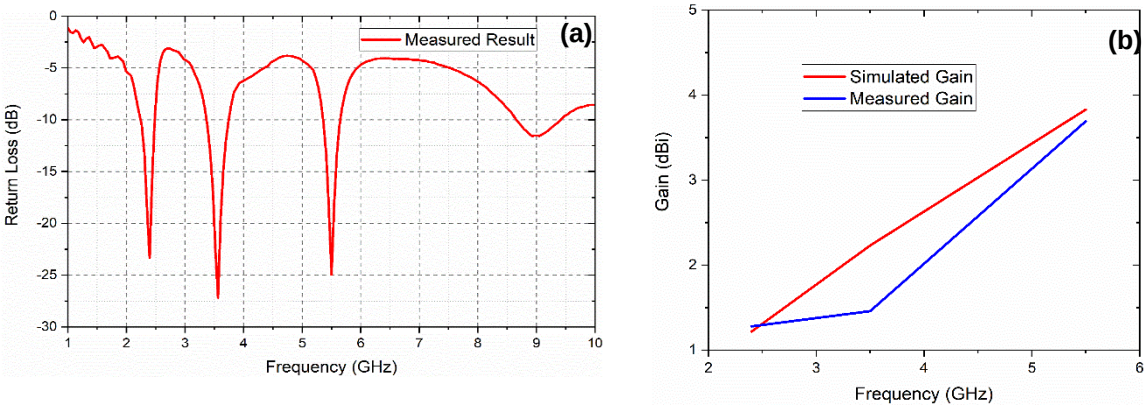

Figure 10. Measurement results of (a) Return loss (b) Gain versus Frequency of the proposed compact triple band antenna

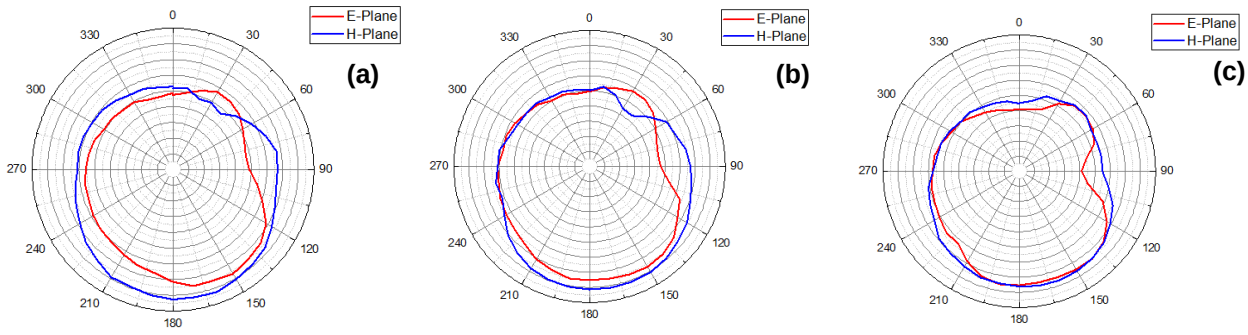

Figure 11. Measured RP for the frequencies **(a)** 2.4 **(b)** 3.5 and **(c)** 5.5 GHz respectively.

Table 3. Comparison parameters with previous literature

References	Operating frequencies	Size (mm^3)	Bandwidth (MHz)	Gain	Material
[18]	0.915, 2.45, 5.8	140 × 60 × 0.78	130, 180, 1550	2.03, 2.45, 4.31	Denim
[19]	0.45, 0.8, 1.4	260 × 100 × 3	-	2.1, 2.7, 3.7	Jeans cotton
[20]	2.4, 3.51, 4.69	80 × 80 × 2	60, 58, 101	1.1, 0.9, 2.1	Leather
[21]	0.9, 1.8	80 × 75 × 1.64	70, 175	7.46, 8.13	Rubber
[22]	2.4, 5.8	41 × 41 × 1.52	91.2. 301.6	4.84, 5.87	Rogers Duroid RO3003
[23]	2,4, 3.45	60 × 60 × 8.72	141.1, 162.2	6.7, 8.9	Taconic TLY-5 and felt
[24]	2.4, 5.8	100 × 100 × 2	118, 218	5.93, 6.02	Felt
[25]	2.4, 5.8	41 × 44 × 1.52	89, 301.6	3.74, 5.13	Rogers RO3003
[26]	2.5, 3.6, 5.5	70 × 70 × 2.1	200, 285, 290	2.2, 0.3, 4.4	Felt
[27]	0.868, 2.45	65 × 60	3, 85	NA, -1.4	Metal on hand gloves
[28]	2.45, 3.45	60 × 60	12, 23	6.7, 8.9	Two-layer substrates include rigid and felt
[29]	2.4,3.32, 3.93, 5.8	60 x 60	90, 190, 230, 570	-0.81, -2.81, -1.16, 2.8	denim
[30]	8	55 x 40	1050	5.2	Wool felt
[31]	2.4, 5	84 x 69	5500	7.2	PF4 foam
[32]	1.8, 2.45, 5.8	60 x 60 x 1	310, 960, 1140	3.7, 5.3, 9.6	denim
Proposed Antenna	2.4, 3.5, 5.5	20 x 50 x 0.254	128, 766, 418	1.28, 1.46, 3.69	Jeans

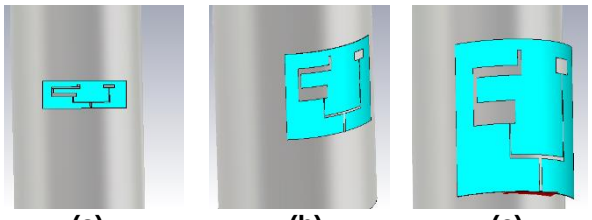

Figure 12. The proposed antenna curvature with and angle of **(a)** 0° **(b)** 30° and **(c)** 60° Respectively

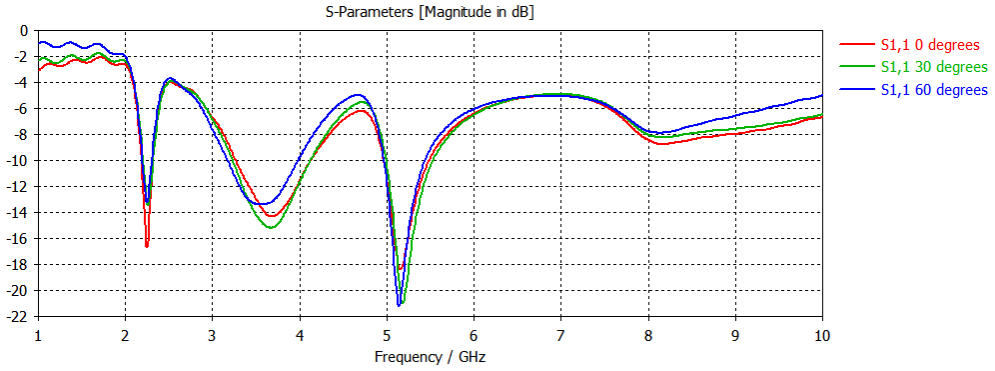

Figure13. S11 characteristics of the proposed triple band antenna on the cylindrical surface.

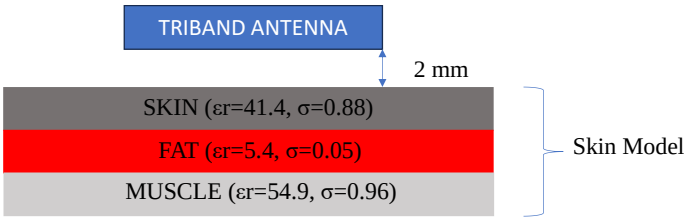

Figure 14. Simulation setup of skin model with 3 layered human body.

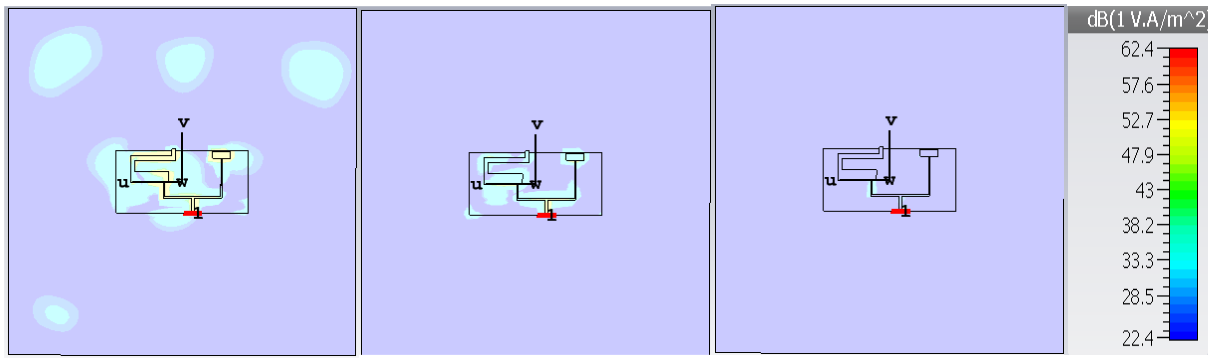

Figure 15. E-field distributions on the skin model for the frequencies **(a)** 2.4 **(b)** 3.5 and **(c)** 5.5 GHz.

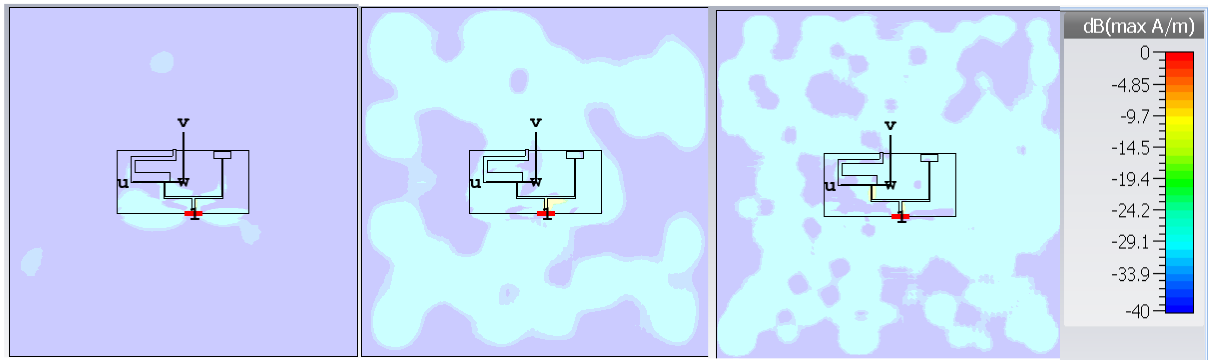

Figure 16. H-field distributions on the skin model for the frequencies **(a)** 2.4 **(b)** 3.5 and **(c)** 5.5 GHz.

From the measured results the resonating frequencies are 2.45, 3.55 and 5.595 GHz respectively. The difference between the simulation and measured results because of the fabrication tolerances and fabricated material properties.

The E-plane and H-plane measured RPs are represented in the figure 11 for the corresponding resonating frequencies, i.e. 2.4, 3.5 and 5.5 GHz respectively.

From the tabulated values in Table 3, a comparison can be drawn between the existing geometry in the literature for the proposed antenna design. A comparison has been drawn regarding operating frequency dimensions with gain material used and, finally, respective applications like other antennas. The proposed geometry also exhibited similar radiation characteristics regarding resonant frequencies, which reported minimal dimensions with a considerable gain and BW. The proposed design has an inherent nature of merging with the decorum of the garment because of its miniaturised dimension. It can be placed in any region as part of the wearable garment. This significant characteristic nature will impact wearable devices, body area networks, healthcare applications, etc.

The proposed antenna is provided enhanced performance in terms of BW, operating frequencies, gain and material used. The proposed compact triple band antenna can be placed in any part of the body.

Bending analysis is the one of the critical parameters in the wearable antenna design, as in this work the bending radius of the cylinder is considered to be 40 mm and the proposed antenna is placed on the cylinder with an angle of 0^o, 30^o and 60^o respectively are represented in the figure 12 and the corresponding simulation result of the S parameters are represented in the figure 13.

The antenna's general characteristics and the frequency of operations are affected by the bending radius. The simulation results are affected by the bending radius and the corresponding results are represented in the figure 13.

Antennas designed for on-body applications operate in close proximity to the human body, where they transmit and receive EM waves. Excessive absorption of EM radiation by human tissue can lead to adverse effects such as tissue heating and potential ionization. To ensure user safety, regulatory bodies such as the IEEE (Institute of Electrical and Electronics Engineers), the ICNIRP (International Commission on Non-Ionizing Radiation Protection), and the FCC (Federal Communications Commission) have established exposure limits. The metric used to quantify the rate at which electromagnetic (EM) energy is absorbed by human tissue is known as the SAR. The simulation model for the proposed triband antenna for SAR analysis is represented in figure 14. The proposed triband antenna is placed above 2 mm from the skin model. The skin model consists of skin, fat and muscle layers represented in the figure 12, the overall size of the skin model considered for the simulation are 100 mm x 100 mm.

The simulation results of E and H-field distributions of the proposed triple band antenna on the skin model is represented in figure 15 and 16 respectively at the frequencies of 2.4, 3.5 and 5.5 GHz. Both the E and H-field radiation effects on the body are very minimal and within the limits. Therefore, the proposed triband antenna for the on-body applications operated at WLAN, WiMAX and IOT frequency bands. The SAR values for the proposed antennas at 2.4, 3.5 and 5.5 GHz are 0.82, 0.79 and 1.1 W/Kg respectively for the peak 1-g.

6. Conclusion

In this paper, the proposed compact textile triple band antenna is operating in the frequencies of 2.3183-2.4465 GHz (BW of 128 MHz), 3.2240 GHz-3.9902 GHz (BW of 766 MHz) and 5.1858-5.6042 GHz (BW of 418 MHz). The antenna demonstrates the excellent bandwidth, S-parameters and radiation characteristics and the size of the proposed compact triple band antenna is 20 mm x 50 mm x 0.254 mm. The simulated and measured results are very close proximity and are in good agreement in terms of the parameters like bandwidth and gain. The measured gain for the antenna is 1.28, 1.46 and 3.69 dBi for WLAN, WiMAX and IOT applications respectively. The proposed antenna is compared with existing antennas highlights its size reduction, improved bandwidth, low cost substrate and other parameters.

References

[1] Z.H. Jiang, D.E. Brocker, P.E. Sieber, D.H. Werner, A compact, low-profile metasurface-enabled antenna for wearable medical body-area network devices. IEEE Transactions on antennas and propagation, 62(8), (2014) 4021-4030. https://doi.org/10.1109/TAP.2014.2327650

[2] S. Seneviratne, Y. Hu, T. Nguyen, G. Lan, S. Khalifa, K. Thilakarathna, M. Hassan, A. Seneviratne. A survey of wearable devices and challenges. IEEE Communications Surveys & Tutorials, 19(4), (2017) 2573-2620. https://doi.org/10.1109/COMST.2017.2731979

[3] A.Y.I. Ashyap, S.H. Bin Dahlan, Z.Z. Abidin, M.I. Abbasi, M.R. Kamarudin, H.A. Majid, M.H. Dahri, M.H. Jamaluddin, M.H.; Alomainy, A. An overview of electromagnetic band-gap integrated wearable antennas. IEEE Access, 8, (2020) 7641–7658. https://doi.org/10.1109/ACCESS.2020.2963997

[4] L.N. Song, Y. Rahmat-Samii. A systematic investigation of rectangular patch antenna bending effects for wearable applications. IEEE Transactions on Antennas and Propagation, 66(5), (2018) 2219–2228. https://doi.org/10.1109/TAP.2018.2809469

[5] R.K. Singh, A. Michel, P. Nepa, A. Salvatore, M. Terraroli, P. Perego. Compact and wearable yagi-like textile antennas for near-field UHF-RFID readers. IEEE Transactions on Antennas and Propagation. 69(3), (2020) 1324–1333. https://doi.org/10.1109/TAP.2020.3030944

[6] K. Agarwal, Y.X. Guo, B. Salam. Wearable AMC backed near-endfire antenna for on-body communications on latex substrate. IEEE Transactions on Components, Packaging and Manufacturing Technology, IEEE, 6(3), (2016) 346-358. https://doi.org/10.1109/TCPMT.2016.2521487

[7] Alemaryeen, S. Noghanian. On-body low-profile textile antenna with artificial magnetic conductor. IEEE Transactions on Antennas and Propagation, IEEE, 67(6), (2019) 3649-3656. https://doi.org/10.1109/TAP.2019.2902632

[8] S. Velan, E.F. Sundarsingh, M. Kanagasabai, A.K. Sarma, C. Raviteja, R. Sivasamy, J.K. Pakkathillam. Dual-band EBG integrated monopole antenna deploying fractal geometry for wearable applications. IEEE antennas and wireless propagation letters, IEEE, 14, (2014) 249-252. https://doi.org/10.1109/LAWP.2014.2360710

[9] G. Gao, B. Hu, S. Wang, C. Yang. Wearable planar inverted-F antenna with stable characteristic and low specific absorption rate. Microwave and Optical Technology Letters, 60(4), (2018) 876-882. https://doi.org/10.1002/mop.31069

[10] Z.H. Jiang, D.E. Brocker, P.E. Sieber, D.H. Werner. A compact, low-profile metasurface-enabled antenna for wearable medical body-area network devices. IEEE Transactions on antennas and propagation, IEEE, 62(8), (2014) 4021-4030. https://doi.org/10.1109/TAP.2014.2327650

[11] T.T. Le, T.Y. Yun. Miniaturization of a dual-band wearable antenna for WBAN applications. IEEE Antennas and Wireless Propagation Letters, IEEE, 19(8), (2020) 1452-1456. https://doi.org/10.1109/LAWP.2020.3005658

[12] M. El Atrash, M.A. Abdalla, H.M. Elhennawy. A wearable dual-band low profile high gain low SAR antenna AMC-backed for WBAN applications. IEEE Transactions on Antennas and Propagation, 67(10), (2019) 6378-6388. https://doi.org/10.1109/TAP.2019.2923058

[13] H.M.A. AlSabbagh, T.A. Elwi, Y. Al-Naiemy, H.M.A. Al-Rizzo. A compact triple-band metamaterial-inspired antenna for wearable applications. Microwave and Optical Technology Letters, 62(2), (2020) 763–777. https://doi.org/10.1002/mop.32067

[14] P. Sambandam, M. Kanagasabai, R. Natarajan, M.G.N. Alsath, S. Palaniswamy. Miniaturized button-like WBAN antenna for off-body communication. IEEE Transactions on Antennas and Propagation, 68(7), (2020) 5228-5235. https://doi.org/10.1109/TAP.2020.2980367

[15] T.T. Le, Y.D. Kim, T.Y. Yun. A triple-band dual-open-ring high-gain high-efficiency antenna for wearable applications. IEEE Access, 9, (2021) 118435-118442 https://doi.org/10.1109/ACCESS.2021.3107605

[16] S.H. Yang, L.Y. Zhang, W.S. Wang, Y.J. Zheng. Flexible tri-band dual-polarized MIMO belt strap antenna toward wearable applications in intelligent internet of medical things. IEEE Transactions on Antennas and Propagation, 70(1), (2021) 197-208. https://doi.org/10.1109/TAP.2021.3098589

[17] A.B. Dey, D. Mitra, W. Arif. Design of CPW fed multiband antenna for wearable wireless body area network applications. International Journal of RF and Microwave Computer-Aided Engineering, 30(12), (2020) e22459. https://doi.org/10.1002/mmce.22459

[18] Mandal, S.K. Parui. Wearable tri-band SIW based antenna on leather substrate. Electronics Letters, 51(20), (2015) 1563–1564. https://doi.org/10.1049/el.2015.2559

[19] M.E. Jalil, M.K.A. Rahim, N.A. Samsuri, N.A. Murad. (2012) Triple band fractal koch antenna for wearable application. In Proceedings of Progress in Electromagnetics Research Symposium, KL, Malaysia.

[20] R. Nagarjun, G. George, D. Thiripurasundari, R. Poonkuzhali, Z.C. Alex. (2013). Design of a triple band planar bow-tie antenna for wearable applications. In 2013 IEEE Conference on Information & Communication Technologies, IEEE, Thuckalay, India, 1185–1189. https://doi.org/10.1109/CICT.2013.6558280

[21] P. Shirvani, F. Khajeh-Khalili, M.H. Neshati, Design investigation of a dual-band wearable antenna for tele-monitoring applications, AEU — International Journal of Electronics and Communications, 138, (2021) 153840. https://doi.org/10.1016/j.aeue.2021.153840

[22] U. Musa, S.M. Shah, H.B.A. Majid, M.K. Rahim, M.S. Yahya, Z. Yunusa, A. Salisu, Z.Z. Abidin, Wearable dual-band frequency reconfigurable patch antenna for WBAN applications. Progress in Electromagnetics Research M, 120, (2023) 95–111. http://dx.doi.org/10.2528/PIERM23060705

[23] T.T. Le, T.Y. Yun. Wearable dual-band high-gain lowSAR antenna for off-body communication. IEEE Antennas and Wireless Propagation Letters, 20(7), (2021) 1175–1179. https://doi.org/10.1109/LAWP.2021.3074641

[24] L. Zhou, S. Fang, X. Jia. Dual-band and dual-polarised circular patch textile antenna for on-/off-body WBAN applications. IET Microwaves, Antennas & Propagation, 14(7), (2020) 643–648. https://doi.org/10.1049/iet-map.2019.1073

[25] U. Musa, S.M. Shah, H.A. Majid, I.A. Mahadi, M.K.A. Rahim, M.S. Yahya, Z.Z. Abidin. Design and analysis of a compact dual-band wearable antenna for WBAN applications, IEEE Access, 11, (2023) 30996–31009. https://doi.org/10.1109/ACCESS.2023.3262298

[26] Shankar, M. Mitra. Triple Band Compact Textile antenna Structure for wearable Applications, Progress in Electromagnetics Research C, 144, (2024) 1-8, 2024. http://dx.doi.org/10.2528/PIERC24031306

[27] R.K. Singh, A. Michel, P. Nepa, A. Salvatore. Wearable dual-band quasi-yagi antenna for UHF-RFID and 2.4 GHz applications. IEEE Journal of Radio Frequency Identification, 4(4), (2020) 420-427.

[28] P. BoseBabu, P.N. Rao, Design of Triple Band Fabric Antenna for WLAN Applications. In 2025 IEEE Wireless Antenna and Microwave Symposium (WAMS), 2025 IEEE Wireless Antenna and Microwave Symposium (WAMS) (2025) 1-5.

https://doi.org/10.1109/WAMS64402.2025.11158476

[29] H. Li, J. Du, X. Yang, S. Gao. Low-profile all-textile multiband microstrip circular patch antenna for WBAN applications. IEEE Antennas and Wireless Propagation Letters, 21(4), (2022) 779-783.https://doi.org/10.1109/LAWP.2022.3146435

[30] Çelenk, N.T. Tokan. All-textile on-body antenna for military applications. IEEE Antennas and Wireless Propagation Letters, IEEE, 21(5), (2022) 1065–1069. https://doi.org/10.1109/LAWP.2022.3159301

[31] P.B. Samal, S.J. Chen, C. Fumeaux. Wearable Textile Multiband Antenna for WBAN Applications. IEEE Transactions on Antennas and Propagation, 71(2), (2023) 1391–1402. https://doi.org/10.1109/TAP.2022.3230550

[32] Sharma, R.N. Tiwari, S. Kumar, S. Sharma, L. Matekovits. A Compact Wearable Textile Antenna for NB-IoT and ISM Band Patient Tracking Applications. Sensors, 24(15), (2024) 5077. https://doi.org/10.3390/s24155077

Authors Contribution Statement

Parisa BoseBabu: Conceptualization, Methodology, Validation, Investigation, Writing - Original Draft. P.A. Nageswara Rao- Formal analysis, Writing - Review & Editing, Supervision. Both the authors read and approved the final version of the manuscript.

Funding

The authors declare that no funds, grants or any other support were received during the preparation of this manuscript.

Competing Interests

The authors declare that there are no conflicts of interest regarding the publication of this manuscript.

Data Availability

The data supporting the findings of this study can be obtained from the corresponding author upon reasonable request.

Has this article screened for similarity?

Yes

About the License